Supplementary Material for

Thermal diffusivity and thermal conductivity of granitoids at 283–988 K and 0.3–1.5 GPa

Huangfei Fu[1, 2], Baohua Zhang[1*], Jianhua Ge[1, 2], Zili Xiong[1, 2] Shuangmeng Zhai[1], Shuangming Shan[1], Heping Li[1]

[1]Key Laboratory for High-Temperature and High-Pressure Study of the Earth's Interior, Institute of Geochemistry, Chinese Academy of Sciences, Guiyang, Guizhou 550081, China
[2]University of Chinese Academy of Sciences, Beijing 100049, China

This supplementary material includes:

(1) Appendix A: Determination of water content
(2) Appendix B: Calculation of geotherms beneath southern Tibet
(3) Figure S1. Unpolarized FT-IR spectra of each constituent mineral in granodiorite before and after the thermal conductivity measurements
(4) Figure S2. Comparison of geotherms modeled for granitic upper-middle crust with solidus curves of muscovite and biotite dehydration (Patiño Douce and Harris 1998). Black dashed lines and dark cyan solid lines represent geotherms calculated from a constant κ ~3.5 $Wm^{-1}K^{-1}$ and a κ as a function of temperature and pressure, respectively. Numbers represent different radiative heat production in $\mu W/m^3$. The heat flux is fixed at 60 mW/m^2 for all models
(5) Supplementary Table 1. Major elements composition analyzed by XRF (in wt %)
(6) Supplementary Table 2. Thermal diffusivity D and thermal conductivity κ of granitoids as a function of temperature and pressure
(7) Supplementary Table 3. Specific heat capacity of individual minerals (Berman and Brown 1985; Clauser 2011). Coefficients for calculating isobaric molar heat capacity from equation: $C_{P,mol} = k_0 + k_1T^{-0.5} + k_2T^{-2} + k_3T^{-3}$ (T in K)
(8) Additional References

Appendix. A Determination of water content

To determine the impact of structural water in constituent mineral phases of natural granitoids on the thermal diffusivity and thermal conductivity, each granitoid sample before and after conductivity experiments was double polished to ~150 μm thickness and measured by Fourier-transformation infrared (FT-IR) spectroscopy using Jasco FTIR-6200 Equipper with IRT-7000 infrared microscope, with 50 × 50 μm aperture size large enough to incorporate dozens of grains. At least five different spots were measured for each constituent mineral using unpolarized light. The water content in samples was calculated by the equation given by Paterson (1982), with an integration range of 2800-4000 cm^{-1}. Fig. S1 shows the representative IR spectra of each constituent mineral in granodiorite before and after the thermal conductivity measurements. The bulk water content in granitoids (Table 1) was estimated from the volume fraction and water content of each constituent mineral.

Appendix. B Calculation of geotherms beneath southern Tibet

In order to better understand the process of melting in southern Tibet, it is necessary to establish a detailed temperature profile of the crust. In this case, the finite element method was applied to solve the Fourier heat conduction in one dimension as follows:

$$\rho C_p \frac{\partial T}{\partial t} = \frac{\partial}{\partial x} k(T,P) \frac{\partial T}{\partial x} + H \qquad (1)$$

where T is the temperature in K, t is the time in years, H is the radiative heat production, and x is the depth in m. To simplify the model, the depth from the upper crust to the lower crust throughout southern Tibet was calculated, and heat conduction was considered as the only mechanism. A typical and moderate value of the surface heat flow (80 mW/m^2) in southern Tibet (Francheteau et al. 1984) was used in our calculation. The density was assumed to be constant at ~2700 kgm^{-3}. The distribution of radiative heat production, both in the horizontal and vertical directions, is poorly constrained in southern Tibet, and thus the constant values of 0.64, 1.21, and 1.65 $\mu W/m^3$ (Huppert and Sparks 1988; Bea 2012; Furlong and Chapman 2013) were employed in this study to roughly represent the low, middle, and high heat production areas of the upper to lower crust, respectively. In this calculation, subcrustal heat flows at 60 km depth were fixed at 50, 25, and 5 mW/m^2 according to the different radiative heat production values applied to ensure that the surface heat flow is maintained at 80 mW/m^2. The heat capacity of silicate minerals is similar, and the pressure dependence of C_P is assumed negligible. Thus, the temperature dependence of heat capacity, $C_P(T)$, from granodiorite sample was applied. Thermal conductivities of granodiorite from the southern Tibet as a function of temperature and pressure fitted from our experimental results were used. For comparison, the model with a constant κ of 3.0 $Wm^{-1}K^{-1}$ was also calculated, and the surface temperature was fixed to 283 K.

Additional References:

Bea, F. (2012) The sources of energy for crustal melting and the geochemistry of heat-producing elements. Lithos, 153, 278–291.

Francheteau, J., Jaupart, C., Shen, X.J., Kang, W.H., Lee, D.L., Bai, J.C.., Wei, H.P., Deng, H.Y. (1984). High heat flow in southern Tibet. Nature, 307(5946), 32–36.

Furlong, K.P., and Chapman, D.S. (2013) Heat flow, heat generation, and the thermal state of the lithosphere. Annual Review of Earth and Planetary Sciences, 41, 385–410.

Huppert, H.E., and Sparks, R.S.J. (1988) The generation of granitic magmas by intrusion of basalt into continental crust. *Journal of* Petrology, **29**, 599–624.

Paterson, M.S., 1982, The determination of hydroxyl by infrared absorption in quartz, silicate glasses and similar materials: Bulletin de Mineralogie, v. 105, p. 20–29.

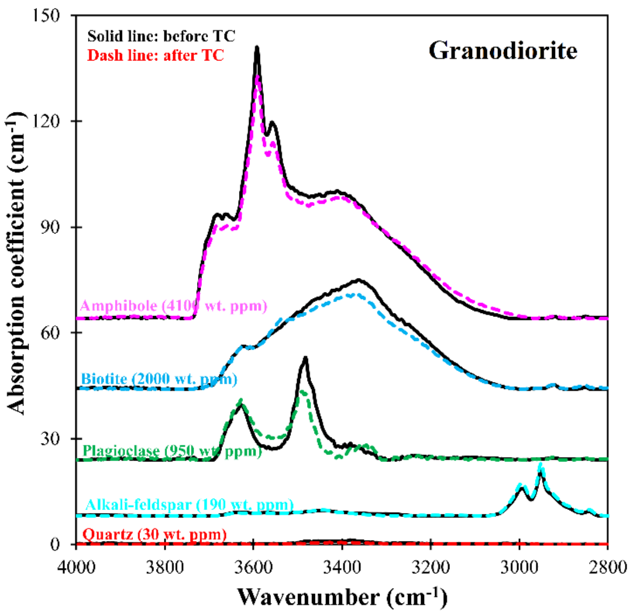

Figure S1. Unpolarized FT-IR spectra of each constituent mineral in granodiorite before and after the thermal conductivity measurements.

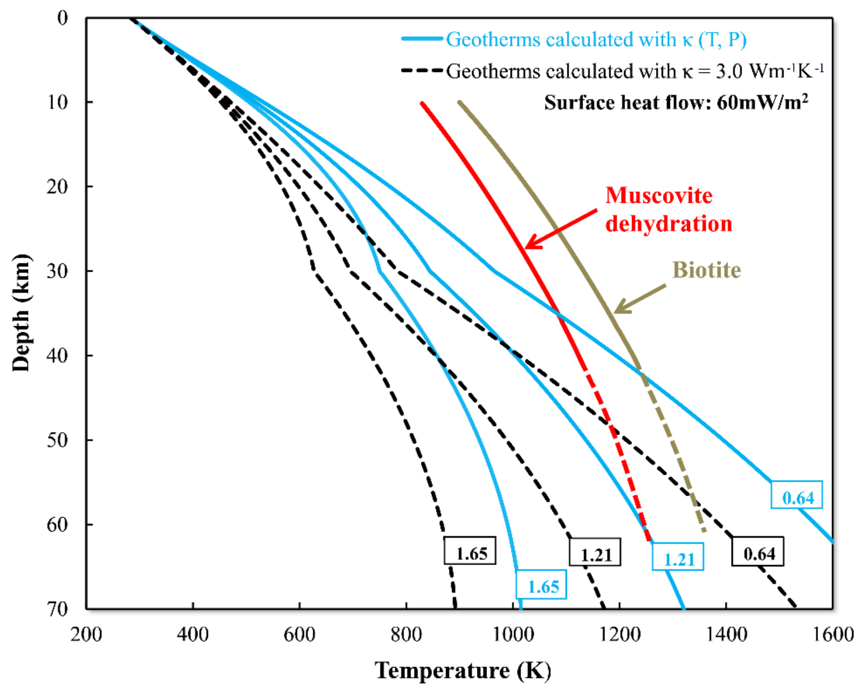

Figure S2. Comparison of geotherms modeled for granitic upper-middle crust with solidus curves of muscovite and biotite dehydration (Patiño Douce and Harris 1998). Black dashed lines and dark cyan solid lines represent geotherms calculated from a constant *κ* ~3.5 $Wm^{-1}K^{-1}$ and a *κ* as a function of temperature and pressure, respectively. Numbers represent different radiative heat production in $\mu W/m^3$. The heat flux is fixed at 60 mW/m^2 for all models.

Supplementary Table 1 Major elements composition analyzed by XRF (in wt %).

	Granodiorite	Monzogranite	Syenogranite	Alkaline granite
SiO_2	65.02 (1.12)	69.09 (1.23)	70.52 (0.98)	73.43 (1.26)
TiO_2	0.57 (0.03)	0.20 (0.02)	0.18 (0.02)	0.08 (0.01)
Al_2O_3	16.94 (0.11)	14.83 (0.14)	14.52 (0.13)	13.64 (0.17)
Fe_2O_3	2.09 (0.04)	1.91 (0.03)	1.24 (0.02)	0.23 (0.06)
MnO	0.08 (0.02)	0.06 (0.01)	0.03 (0.01)	-
MgO	1.98 (0.03)	0.45 (0.02)	0.35 (0.01)	0.12 (0.02)
CaO	4.80 (0.13)	2.37 (0.08)	1.33 (0.07)	0.59 (0.03)
Na_2O	3.46 (0.15)	3.98 (0.12)	4.70 (0.09)	4.29 (0.10)
K_2O	2.52 (0.08)	3.26 (0.07)	3.86 (0.11)	4.60 (0.13)
P_2O_5	0.16 (0.02)	0.09 (0.01)	0.06 (0.01)	0.05 (0.01)
LOI	1.65 (0.02)	1.73 (0.04)	1.44 (0.03)	1.79 (0.05)
Total	99.27 (0.23)	97.98 (0.56)	98.24 (0.47)	98.81 (0.52)

Supplementary Table 2 Thermal diffusivity *D* and thermal conductivity *κ* of granitoids as a function of temperature and pressure.

Granodiorite (*L* = 2.89 mm)				**Monzogranite** (*L* = 2.78 mm)				**Syenogranite** (*L* = 1.98 mm)				**Alkaline granite** (*L* = 2.65 mm)			
T (K)	P (GPa)	D ($mm^2 s^{-1}$)	κ ($Wm^{-1} K^{-1}$)	T (K)	P (GPa)	D ($mm^2 s^{-1}$)	κ ($Wm^{-1} K^{-1}$)	T (K)	P (GPa)	D ($mm^2 s^{-1}$)	κ ($Wm^{-1} K^{-1}$)	T (K)	P (GPa)	D ($mm^2 s^{-1}$)	κ ($Wm^{-1} K^{-1}$)
283	0.3	1.392 (70)	2.834 (98)	283	0.5	1.643 (82)	3.373 (94)	283	0.3	2.006 (100)	4.169 (122)	283	0.5	1.944(97)	3.936 (110)
283	0.5	1.464 (73)	3.006 (84)	320	0.5	1.430(74)	3.128 (90)	283	0.5	2.083 (104)	4.244 (119)	310	0.5	1.726 (89)	3.618 (104)
328	0.5	1.223 (63)	2.537 (73)	345	0.5	1.346 (71)	3.013 (89)	316	0.5	1.871 (96)	3.918 (112)	366	0.5	1.443 (76)	3.184 (94)
372	0.5	1.081 (57)	2.305 (68)	389	0.5	1.146 (62)	2.800 (85)	371	0.5	1.423 (75)	3.386(100)	419	0.5	1.327 (72)	2.951 (89)
425	0.5	0.977 (52)	2.250 (67)	538	0.5	0.978 (55)	2.458 (77)	469	0.5	1.214 (65)	3.119 (94)	496	0.5	1.174 (65)	2.842 (88)
476	0.5	0.904 (49)	2.232 (68)	674	0.5	0.807 (46)	2.256 (73)	627	0.5	0.908 (50)	2.619 (81)	614	0.5	1.018 (58)	2.741 (90)
581	0.5	0.864 (48)	2.166 (68)	762	0.5	0.735 (43)	2.252 (74)	699	0.5	0.857 (48)	2.510 (79)	775	0.5	0.900 (52)	2.582 (92)
712	0.5	0.771 (44)	2.166 (69)	885	0.5	0.743 (45)	2.241 (76)	785	0.5	0.788 (45)	2.343 (75)	883	0.5	0.859 (51)	2.515 (95)
843	0.5	0.765 (44)	2.156 (71)	283	0.75	1.713 (86)	3.423 (130)	921	0.5	0.724 (43)	2.311 (76)	283	1.0	2.089 (104)	4.215 (135)
957	0.5	0.691 (41)	2.167 (70)	283	1.0	1.762 (88)	3.590 (121)	283	1.0	2.170 (108)	4.330 (143)				
283	1.0	1.527 (76)	3.190 (113)					507§	0.5§	1.146 (57)§	2.861 (200)§				
425§	0.5§	0.983 (49)§	2.229 (156)§					719§	0.5§	0.856 (43)§	2.405 (168)§				
515§	0.5§	0.907 (45)§	2.205 (154)§												
655§	0.5§	0.808 (40)§	2.183 (153)§												
806§	0.5§	0.756 (38)§	2.144 (150)§												

Granodiorite* (*L* = 1.79 mm)							**Monzogranite*** (*L* = 1.97 mm)								
	0.5 GPa		1.0 GPa		1.5 GPa		0.5 GPa			1.0 GPa			1.5 GPa		
T (K)	D ($mm^2 s^{-1}$)	κ ($Wm^{-1} K^{-1}$)	D ($mm^2 s^{-1}$)	κ ($Wm^{-1} K^{-1}$)	D ($mm^2 s^{-1}$)	κ ($Wm^{-1} K^{-1}$)	T (K)	D ($mm^2 s^{-1}$)	κ ($Wm^{-1} K^{-1}$)	T (K)	D ($mm^2 s^{-1}$)	κ ($Wm^{-1} K^{-1}$)	T (K)	D ($mm^2 s^{-1}$)	κ ($Wm^{-1} K^{-1}$)
283	1.435 (73)	2.947 (94)	1.581 (82)	3.254 (110)	1.778 (97)	3.512 (119)	283	1.685 (82)	3.433 (107)	283	1.841 (110)	3.702 (110)	283	1.976 (97)	3.987 (119)
329	1.258 (63)	2.571 (90)	1.354 (74)	2.901 (104)	1.525 (89)	3.221 (112)	316	1.482 (74)	3.249 (102)	329	1.577 (104)	3.455 (104)	327	1.759 (89)	3.720 (112)
378	1.116 (57)	2.443 (89)	1.213 (71)	2.632 (94)	1.364 (76)	2.937 (100)	360	1.347 (71)	3.072 (96)	372	1.434 (97)	3.243 (94)	373	1.508 (76)	3.427 (100)
431	1.033 (52)	2.239 (85)	1.077 (62)	2.532 (89)	1.184 (72)	2.786 (94)	411	1.158 (62)	2.911 (94)	421	1.281 (77)	3.058 (89)	433	1.425 (72)	3.330 (94)
483	0.933 (49)	2.169 (77)	1.005 (55)	2.295 (88)	1.086 (65)	2.449 (81)	464	1.080 (55)	2.823 (90)	476	1.122 (75)	2.960 (88)	486	1.264 (65)	3.173 (81)

543	0.894 (48)	2.108 (73)	0.931 (46)	2.209 (89)	1.009 (56)	2.312 (79)	542	0.961 (46)	2.723 (89)	518	1.050 (62)	2.856 (90)	543	1.097 (58)	3.013 (79)
600	0.822 (44)	2.121 (68)	0.877 (45)	2.150 (85)	0.961 (47)	2.298 (77)	610	0.916 (52)	2.702 (85)	576	0.988 (55)	2.813 (92)	598	1.059 (52)	2.904 (75)
663	0.805 (44)	2.079 (67)	0.839 (44)	2.109 (77)	0.888 (45)	2.258 (76)	688	0.852 (45)	2.528 (77)	630	0.951 (57)	2.709 (95)	671	0.972 (51)	2.854 (76)
721	0.786 (44)	2.057 (68)	0.819 (44)	2.146 (75)	0.860 (46)	2.278 (75)	767	0.812 (58)	2.447 (73)	753	0884 (53)	2.610 (81)	758	0.928 (43)	2.761 (72)
781	0.777 (43)	2.032 (68)	0.797 (44)	2.104 (75)	0.833 (43)	2.231 (72)	816	0.782 (52)	2.469 (74)	806	0.843 (45)	2.553 (79)	836	0.909 (46)	2.753 (74)
838	0.755 (43)	2.067 (69)	0.777 (44)	2.087 (77)	0.817 (46)	2.216 (77)	861	0.767 (51)	2.387 (76)	923	0.810(47)	2.536 (81)	908	0.877 (43)	2.685 (72)
896	0.739 (41)	2.035 (71)	0.745 (43)	2.070 (77)	0.775 (43)	2.235 (75)	933	0.746 (43)	2.421 (77)	973	0.794 (51)	2.533 (79)	971	0.842 (45)	2.703 (74)
958	0.726 (44)	2.042 (70)	0.734 (42)	2.095 (75)	0.793 (45)	2.200 (74)	988	0.732 (52)	2.459 (78)						

L is the thickness of granitoid sample; § Measurement during cooling; *Thermal diffusivity D and thermal conductivity κ of granodiorite and monzogranite were remeasured under 0.5, 1.0 and 1.5 GPa, respectively, with various temperature (283-988 K).

Supplementary Table 3 Specific heat capacity of individual minerals (Berman and Brown 1985; Clauser 2011). Coefficients for calculating isobaric molar heat capacity from equation: $C_{P,mol} = k_0 + k_1 T^{-0.5} + k_2 T^{-2} + k_3 T^{-3}$ (T in K).

Mineral	Chemical composition	k_0 (J mol^{-1}K^{-1})	$k_1 \times 10^{-2}$ (J mol^{-1}K$^{-1/2}$)	$k_2 \times 10^{-5}$ (J mol^{-1}K^{1})	$k_3 \times 10^{-7}$ (J mol^{-1}K^{2})	T(K)
Albite	$NaAlSi_3O_8$	393.64	-24.155	-78.928	107.064	250–1373
Potassium feldspar	$KAlSi_3O_8$	381.37	-19.411	-120.373	183.643	250–997
Anorthite	$CaAl_2Si_2O_8$	439.37	-37.341	0.0	31.702	292–1373
Quartz	SiO_2	80.01	-2.403	-35.467	49.157	250–1676
Muscovite	$KAl_3Si_3O_{10}(OH)_2$	651.49	-38.732	-185.232	274.247	257–967
Tremolite	$Ca_2Mg_5Si_8O_{22}(OH)_2$	1141.97	-37.937	-420.313	548.553	250–680

Biotite: $C_{P,mol} = 583.586 + 0.075246 \times T - 3420.60 \times T^{-0.5} - 4455100 \times T^{-2}$ (250–1000 K) (Hemingway and Robie 1990)